


**Renormalization group theory of percolation on pseudofractal simplicial and cell complexes**Hanlin Sun *School of Mathematical Sciences, Queen Mary University of London, London E1 4NS, United Kingdom*

Robert M. Ziff

*Center for the Study of Complex Systems and Department of Chemical Engineering, University of Michigan, Ann Arbor, Michigan 48109-2800, USA*Ginestra Bianconi *The Alan Turing Institute, 96 Euston Rd, London NW1 2DB, United Kingdom and School of Mathematical Sciences, Queen Mary University of London, London E1 4NS, United Kingdom*

(Received 6 May 2020; accepted 24 June 2020; published 14 July 2020)

Simplicial complexes are gaining increasing scientific attention as they are generalized network structures that can represent the many-body interactions existing in complex systems ranging from the brain to high-order social networks. Simplicial complexes are formed by simplicies, such as nodes, links, triangles, and so on. Cell complexes further extend these generalized network structures as they are formed by regular polytopes, such as squares, pentagons, etc. Pseudofractal simplicial and cell complexes are a major example of generalized network structures and they can be obtained by gluing two-dimensional  $m$ -polygons ( $m = 3$  triangles,  $m = 4$  squares,  $m = 5$  pentagons, etc.) along their links according to a simple iterative rule. Here we investigate the interplay between the topology of pseudofractal simplicial and cell complexes and their dynamics by characterizing the critical properties of link percolation defined on these structures. By using the renormalization group we show that the pseudofractal simplicial and cell complexes have a continuous percolation threshold at  $p_c = 0$ . When the pseudofractal structure is formed by polygons of the same size  $m$ , the transition is characterized by an exponential suppression of the order parameter  $P_\infty$  that depends on the number of sides  $m$  of the polygons forming the pseudofractal cell complex, i.e.,  $P_\infty \propto p \exp(-\alpha/p^{m-2})$ . Here these results are also generalized to random pseudofractal cell complexes formed by polygons of different number of sides  $m$ .

DOI: [10.1103/PhysRevE.102.012308](https://doi.org/10.1103/PhysRevE.102.012308)**I. INTRODUCTION**

Simplicial and cell complexes [1,2] are generalized network structures capturing the many-body interactions existing in complex systems such as brain networks [3–5], social networks [6–8], and complex materials [9,10]. Simplicial and cell complexes are not only formed by nodes and links like networks, but they are also formed by higher-dimensional simplexes and polytopes such as triangles, squares, pentagons, etc. Being formed by geometrical and topological building blocks simplicial complexes are ideal structures to study network geometry [11–13]. Moreover, simplicial complexes are key to investigate the role that network geometry and many-body interactions have on dynamics. Among the vast variety of dynamical processes that are starting to be investigated on simplicial complexes we mention percolation [14–17], synchronization [18–23], epidemic spreading [7,24], Gaussian models [10,25,26], and random walks [27,28]. The vast majority of hierarchical networks studied in statistical mechanics and network theory literature is formed by the skeleton of simplicial and cell complexes (i.e., the network formed by its nodes and links). Examples range from the diamond network of Migdal and Kadanoff [29,30] to the hyperbolic Farey graphs that have been shown to display a discontinuous

percolation phase transition in Ref. [31]. These networks are well suited to perform exact real-space renormalization group (RG) calculations. Using RG theory there has been very important progress in characterizing the critical properties of percolation [14–16,31–36], spin (Ising and Potts) models [37–40], and Gaussian models [25,26] in these structures. In particular in Refs. [15,16] the robustness of the result obtained by Boettcher, Singh and Ziff in Ref. [31] has been investigated by considering more general simplicial and cell complexes. It has been found that two-dimensional simplicial and cell complexes, i.e., simplicial and cell complexes build by gluing two-dimensional polygons along their links, can display a large variety of critical behaviors for the order parameter of link percolation. Here we extend this line of research and we characterize the link percolation transition to random pseudofractal simplicial and cell complexes. Pseudofractal simplicial complexes have been originally proposed as deterministic models for complex networks in Ref. [41]. Link percolation on these deterministic pseudofractal networks has been discussed previously in Ref. [42]. Here, however, we provide a more extensive treatment of the problem and are able to show that the critical percolation properties of the deterministic pseudofractal simplicial complex differs from the percolation properties of the deterministic

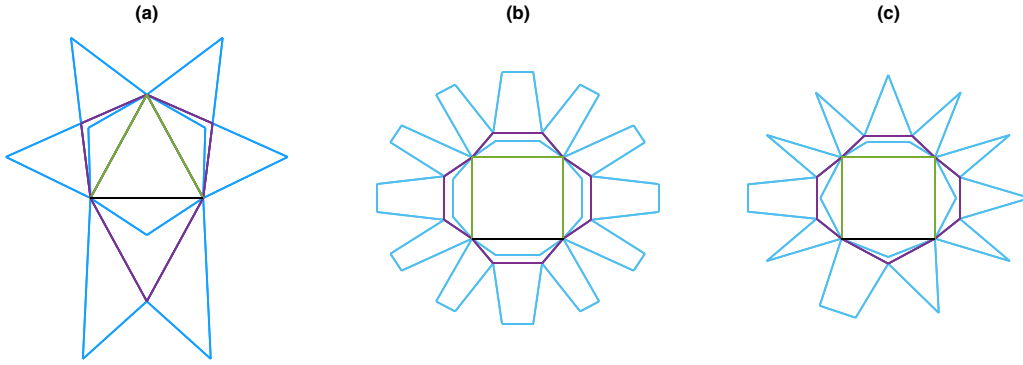


FIG. 1. Examples of pseudofractal simplicial and cell complexes represented at iteration  $n = 3$ . Panel (a) shows a deterministic pseudofractal simplicial complex with  $m = 3$ , panel (b) shows a deterministic pseudofractal cell complex with  $m = 4$ , panel (c) shows a random pseudofractal cell complex with  $q_3 = q_4 = 1/2$ . The different colors indicate the different iterations:  $n = 0$  (black),  $n = 1$  (green),  $n = 2$  (purple),  $n = 3$  (cyan).

pseudofractal cell complex and the random pseudofractal simplicial complexes. Indeed our work shows that for the deterministic pseudofractal simplicial complexes formed by  $m$ -polygons, the phase transition is at  $p_c = 0$  and the order parameter behaves as

$$P_\infty \propto p \exp(-\alpha/p^{m-2}), \quad (1)$$

where  $\alpha$  is a constant. Therefore, the exponential suppression goes like  $1/p$  for  $m = 3$  as obtained by Ref. [42] but goes like  $1/p^{m-2}$  for  $m > 3$ . On a side note we mention also that our derivation also captures the factor  $p$  in Eq. (1) not discussed in Ref. [41]. Finally, for random pseudofractal simplicial complexes we show that the critical behavior is dictated by the smallest value of  $m$  of the polygons of the cell complex. This results shows that the critical properties depend on the type of 2-dimensional cells forming the building block of the cell complex weakening the universality of the critical behaviour.

The paper is structured as follows: in Sec. II we describe the main properties of the random pseudofractal cell complexes studied in this work; in Sec. III we introduce link percolation on pseudofractal cell complexes, we derive the iterative equations for the linking probability defining the RG equations, and we derive the expression for the generating functions and the for the order parameter in terms of the linking probability, in Sec. IV we discuss the RG flow, in Sec. V we derive the critical behavior of the order parameter, finally in Sec. VI we provide the conclusions.

## II. RANDOM PSEUDOFRACTAL SIMPLICIAL AND CELL COMPLEXES

The pseudofractal simplicial complex [41] is constructed iteratively starting at iteration  $n = 0$  from a single link. At each time  $n \geq 1$  we attach a triangle to every link introduced at iteration  $0 \leq n' < n$ . This construction can be generalized by considering a random cell complex formed by regular  $m$ -polygons with different  $m \geq 3$ . We start at iteration  $n = 0$  from an initial link. At each iteration  $n \geq 1$  we glue a  $m$ -polygon to every link of the cell complex introduced at iteration  $0 \leq n' < n$  with  $m \geq 3$  drawn from a  $q_m$  distribution. It is easy to show that at iteration  $n$  the expected number of

nodes  $\bar{N}_n$  and links  $\bar{L}_n$  are given by

$$\bar{N}_n = 2 + \frac{\langle m \rangle - 2}{\langle m \rangle - 1} (\langle m \rangle^n - 1), \quad \bar{L}_n = \langle m \rangle^n, \quad (2)$$

where  $\langle m \rangle = \sum_{m \geq 3} m q_m$ . In the following, we will refer to these generalized network structures as random cell complexes. However, for  $q_m = \delta_{m,3}$  the random pseudofractal cell complex reduces to the pseudofractal simplicial complex [see Fig. 1(a)]. Moreover, for  $q_{m'} = \delta_{m',m}$  and  $m > 3$  we obtain a deterministic cell complex formed by gluing only  $m$ -polygons [see Fig. 1(b) for an example of a deterministic cell complex with  $m = 4$ ]. Only if the distribution  $q_m$  is not a Kronecker delta, the model reduces to a genuine random cell complex [see Fig. 1(c) for an example of a random cell complex with  $q_3 = q_4 = 1/2$ ].

## III. LINK PERCOLATION ON PSEUDOFRACTAL SIMPLICIAL AND CELL COMPLEXES

### A. Link probability

In this paper we investigate the critical properties of link percolation on pseudofractal cell complexes. We assume that each link is retained with probability  $p$ . It follows that each link is removed with probability  $q = 1 - p$ . To study link percolation on pseudofractal cell complexes we first derive the RG equations for the linking probability  $T_n$  that the two initial nodes of the pseudofractal cell complex are linked at iteration  $n$ . At iteration  $n = 0$  the two initial nodes are connected if the link between them is present, therefore  $T_0 = p$ . At iteration  $n \geq 0$  the two initial nodes are connected by a path except if the initial link is not present and the two nodes are not connected by any path passing through any of the  $m$ -polygons glued to initial link at different iterations. Therefore, for a deterministic pseudofractal cell complex with  $q_{m'} = \delta_{m',m}$  we obtain

$$T_{n+1} = 1 - (1 - p) \prod_{j=0}^n (1 - T_j^{m-1}), \quad (3)$$

with initial condition  $T_0 = p$ . For the random pseudofractal cell complexes the iterative equations determining  $\{T_n\}_{n \geq 0}$  needs to take into account the randomness of  $m$ . It is therefore

immediate to show that we have

$$T_{n+1} = 1 - (1 - p) \left[ \prod_{j=0}^n (1 - Q(T_j)) \right], \quad (4)$$

where  $Q(T)$  is given by

$$Q(T) = \sum_{m \geq 3} q_m T^{m-1}, \quad (5)$$

with  $T_0 = p$ . This recursive set of equations can be also written as

$$T_{n+1} = 1 - (1 - T_n)[1 - Q(T_n)]. \quad (6)$$

with  $T_0 = p$ . The fixed point solutions are only

$$T^* = 0, \quad T^* = 1. \quad (7)$$

For any  $p > 0$  the recursive equations go to the fixed point  $T^* = 1$ . Instead exactly at  $p = 0$  the steady state solution is  $T^* = 0$ . Therefore, for any link probability  $p > 0$  the percolation probability of an infinite network is  $T^* = 1$ . Indeed the RG flow described by Eq. (6) starts with  $T_0 = p$  and in the limit  $n \rightarrow \infty$  reaches

$$\lim_{n \rightarrow \infty} T_n = T^* = \begin{cases} 1 & \text{if } p > 0, \\ 0 & \text{if } p = 0. \end{cases} \quad (8)$$

Therefore, the (upper) percolation threshold is

$$p_c = 0. \quad (9)$$

At  $p = p_c = 0$  the percolation probability is

$$T_c = 0. \quad (10)$$

### B. Generating function

In this paragraph we derive the expression for the generating function  $\hat{T}_n(x)$  and  $\hat{S}_n(x, y)$  which are key to determine the properties of the link percolation in the pseudofractal cell complexes. The function  $\hat{T}_n(x)$  is the generating function of the number of nodes in the connected component linked to both initial nodes of the considered random branching network. The function  $\hat{S}_n(x, y)$  is the generating function of the sizes of the two connected components linked exclusively to one of the two initial nodes of the same network. These generating functions are defined as

$$\hat{T}_n(x) = \sum_{\ell=0}^{\infty} t_n(\ell) x^\ell, \quad \hat{S}_n(x, y) = \sum_{\ell, \bar{\ell}} s_n(\ell, \bar{\ell}) x^\ell y^{\bar{\ell}}, \quad (11)$$

where  $t_n(\ell)$  indicates the probability that  $\ell$  nodes are connected to the two initial nodes and  $s_n(\ell, \bar{\ell})$  indicates the joint probability that  $\ell$  nodes are connected exclusively to one initial node and  $\bar{\ell}$  nodes are connected exclusively to other initial node. Therefore, for every value of  $n$ ,  $t_n(\ell)$  and  $s_n(\ell, \bar{\ell})$  obey the normalization condition

$$\sum_{\ell=0}^{\infty} t_n(\ell) + \sum_{\ell=0}^{\infty} \sum_{\bar{\ell}=0}^{\infty} s_n(\ell, \bar{\ell}) = 1, \quad (12)$$

which implies

$$\hat{T}_n(1) + \hat{S}_n(1, 1) = 1. \quad (13)$$



FIG. 2. Diagrammatic representation of generating functions  $\hat{T}_n(x)$  (a) and  $\hat{S}_n(x, y)$  (b). Filled areas indicate connected components that either connect to both end nodes [ $\hat{T}_n(x)$ ] or connect to a single end node [ $\hat{S}_n(x, y)$ ].

The generating functions at iteration  $n = 0$  are given by

$$\hat{T}_0(x) = p, \quad \hat{S}_0(x, y) = 1 - p, \quad (14)$$

because initially the two nodes can be either connected by a link (which occurs with probability  $p$ ) or not connected by a link (which occurs with probability  $1 - p$ ). In both cases the two initial nodes are not connected to any other node, so  $t_n(0) = p$  and  $t_n(\ell) = 0$ , for all  $\ell > 0$ ; similarly,  $s_n(0, 0) = 1 - p$  and  $s_n(\ell, \bar{\ell}) = 0$ , for all  $(\ell, \bar{\ell}) \neq (0, 0)$ .

Our aim is to write a set of recursive equations for  $\hat{T}_{n+1}(x)$  and  $\hat{S}_{n+1}(x, y)$  expressing the generating functions at iteration  $n + 1$  given the expression of the generating functions at previous generations. To this end we follow the diagrammatic representation of the generating functions  $\hat{T}_n(x)$  and  $\hat{S}_n(x, y)$ , already introduced in Refs. [15,16,31]. In particular, we represent  $\hat{T}_n(x)$  and  $\hat{S}_n(x, y)$  with the diagrams presented in Fig. 2.

At iteration  $n + 1$  the initial link will be incident to  $n + 1$  polygons added subsequently at each iteration. The polygon added at iteration  $n + 1 - j$  with  $0 \leq j \leq n$  has links whose statistical properties are equivalent to the one of the initial link at iteration  $j$ . If we consider a single polygon added at iteration  $n + 1 - j$ , its links will connect the two initial nodes to other nodes of the cell complex added at later generations, and these nodes will not be reachable by following links that branch out from other polygons. The polygon added at iteration  $n + 1 - j$  will contribute to the generating functions  $\hat{T}_{n+1}(x)$  and  $\hat{S}_{n+1}(x, y)$  with terms that can be expressed diagrammatically as described in Fig. 3(a) for a  $m$ -polygon with  $m = 4$ . Only one of these diagrams, i.e., the diagram corresponding to  $x^{m-2} T_j^{m-1}$  (diagram (a) in Fig. 3) will guarantee connectivity of the two end nodes. Therefore, the diagram in Fig. 3(a) and its counterpart diagrams for polygons of different number of sides, cannot contribute to  $\hat{S}_n(x, y)$ . However, since the initial link at iteration  $n$  is connected to  $n$  polygons and connectivity can be guaranteed by the initial link or, when this link is removed, by any one of the polygons connected to the initial link, all diagrams contribute to  $\hat{T}_{n+1}(x)$ .

To calculate the generating function  $\hat{S}_n(x, y)$  we need to impose that the initial nodes are not directly connected, i.e., for every polygons we need to consider only the contributions from diagrams that do not guarantee connectivity (diagrams (b–h) of Fig. 3). In this way, for a deterministic pseudofractal cell complex we obtain

$$\begin{aligned} \hat{S}_{n+1}(x, y) &= (1 - p) \prod_{j=0}^n \left[ \sum_{r=0}^{m-2} x^r y^{m-2-r} \hat{T}_j^r(x) \hat{S}_j(x, y) \hat{T}_j^{m-2-r}(y) \right. \\ &\quad \left. + \sum_{s=0}^{m-3} \sum_{r=0}^s x^r y^{s-r} \hat{T}_j^r(x) \hat{S}_j(x, 1) \hat{S}_j(y, 1) \hat{T}_j^{s-r}(y) \right]. \end{aligned} \quad (15)$$

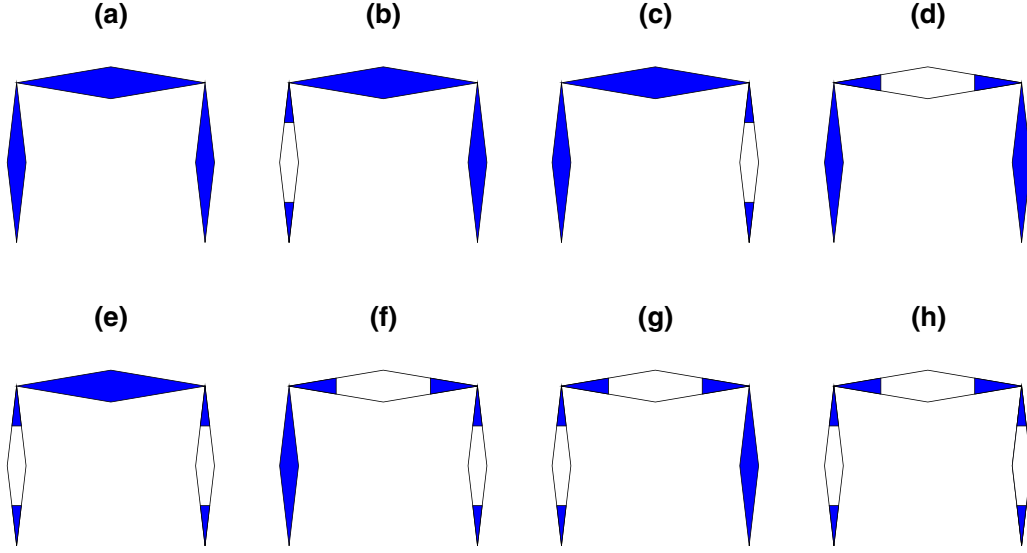


FIG. 3. The diagrams coming from a single  $m$ -polygon added at iteration  $n + 1 - j$  with  $m = 4$  are shown. These diagrams represent terms that contribute to  $\hat{T}_{n+1}(x)$  and  $\hat{S}_{n+1}(x, y)$ . Diagram (a) contributes exclusively to  $\hat{T}_{n+1}(x)$  with a term  $x^2 \hat{T}_j^3$ , diagrams (b–h) contribute both to  $\hat{T}_{n+1}(x)$  and  $\hat{S}_{n+1}(x, y)$ . The diagrams (b–h) contribute to  $\hat{T}_{n+1}(x)$  under the assumption that both initial nodes are connected either by the initial link or by polygons added at different generations. The contribution of the diagrams (b–h) to  $\hat{T}_{n+1}(x)$  are: (b, c, and d)  $x^2 \hat{T}_j^2(x) \hat{S}_n(x, x)$ ; (e) and (h)  $\hat{S}_j^2(x, 1)$ ; (f, g)  $x \hat{T}_j(x) \hat{S}_j^2(x, 1)$ . The diagrams (b–h) contribute to  $\hat{S}_{n+1}(x, y)$  under the assumption that the two initial nodes not connected by the initial link and by any other polygon added at different generations. The contribution of the diagrams (b–h) to  $\hat{S}_{n+1}(x, y)$  are: (b)  $y^2 \hat{T}_j^2(y) \hat{S}_n(x, y)$ ; (c)  $x^2 \hat{T}_j^2(x) \hat{S}_n(x, y)$ ; (d)  $xy \hat{T}_j(x) \hat{T}_j(y) \hat{S}_n(x, y)$ ; (e, h)  $\hat{S}_j(x, 1) \hat{S}_j(y, 1)$ ; (f, g)  $x \hat{T}_j(x) \hat{S}_j(x, 1) \hat{S}_j(y, 1)$ ; (g)  $y \hat{T}_j(y) \hat{S}_j(x, 1) \hat{S}_j(y, 1)$ .

The derivation of the recursive equation for  $\hat{T}_{n+1}(x)$  is slightly more complex. In fact, to guarantee that  $\hat{T}_{n+1}(x)$  is the generating function of the connected component connected to both initial nodes, we need to impose connectivity. As noted before, it is sufficient that the initial link guarantees connectedness or, when this link is removed, it is sufficient that a single polygon contributes for the connectedness of the two initial nodes. Therefore, we express  $T_{n+1}(x)$  as the

difference between two terms. The first term considers, for each polygon the contribution of all diagrams (the one that guarantee connectedness and the one that do not). The second term considers for each polygons only the terms that do not guarantee connectedness, i.e. removes from the first term the contribution coming from disconnected configurations. In this way for a deterministic pseudofractal cell complex we obtain

$$\hat{T}_{n+1}(x) = \prod_{j=0}^n \left[ x^{m-2} \hat{T}_j^{m-1}(x) + (m-1)x^{m-2} \hat{T}_j^{m-2}(x) S_j(x, x) + \sum_{s=0}^{m-3} (s+1)x^s \hat{T}_j^s(x) \hat{S}_j(x, 1) \hat{S}_n(1, x) \right] \\ - (1-p) \prod_{j=0}^n \left[ (m-1)x^{m-2} \hat{T}_j^{m-2}(x) S_j(x, x) + \sum_{s=0}^{m-3} (s+1)x^s \hat{T}_j^s(x) \hat{S}_j(x, 1) \hat{S}_j(1, x) \right].$$

For a random pseudofractal cell complex we can generalize these equations obtaining for  $\hat{T}_n(x)$  and  $\hat{S}_n(x, y)$  the recursion

$$\hat{S}_{n+1}(x, y) = (1-p) \prod_{j=0}^n \left\{ \sum_{m \geq 3} q_m \left[ \sum_{r=0}^{m-2} x^r y^{m-2-r} \hat{T}_j^r(x) \hat{S}_j(x, y) \hat{T}_j^{m-2-r}(y) + \sum_{s=0}^{m-3} \sum_{r=0}^s x^r y^{s-r} \hat{T}_j^r(x) \hat{S}_j(x, 1) \hat{S}_j(y, 1) \hat{T}_j^{s-r}(y) \right] \right\}, \\ \hat{T}_{n+1}(x) = \prod_{j=0}^n \left\{ \sum_{m \geq 3} q_m \left[ x^{m-2} \hat{T}_j^{m-1}(x) + (m-1)x^{m-2} \hat{T}_j^{m-2}(x) S_j(x, x) + \sum_{s=0}^{m-3} (s+1)x^s \hat{T}_j^s(x) \hat{S}_j(x, 1) \hat{S}_n(1, x) \right] \right\} \\ - (1-p) \prod_{j=0}^n \left\{ \sum_{m \geq 3} q_m \left[ (m-1)x^{m-2} \hat{T}_j^{m-2}(x) S_j(x, x) + \sum_{s=0}^{m-3} (s+1)x^s \hat{T}_j^s(x) \hat{S}_j(x, 1) \hat{S}_j(1, x) \right] \right\},$$

with initial conditions  $\hat{T}_0(x) = 1 - \hat{S}_0(x, y) = p$ .

We are particularly interested in the generating function  $\hat{T}_n(x)$  whose derivative calculated for  $x = 1$  gives the expected size of the giant component. The generating function  $\hat{T}_{n+1}(x)$  depends on the generating functions  $\hat{T}_j(x)$  and the functions

$\hat{\Sigma}_j(x) = \hat{S}_j(x, x)$ , and  $\hat{S}_j(x) = \hat{S}_j(1, x)$  at iterations  $0 \leq j \leq n$ . From the above equations for  $\hat{T}_{n+1}(x)$  and  $S_{n+1}(x, y)$  we can deduce directly the set of recursive equations for  $\hat{T}_{n+1}(x)$ ,  $\hat{\Sigma}_{n+1}(x)$ , and  $\hat{S}_{n+1}(x)$  which read

$$\begin{aligned}\hat{T}_{n+1}(x) &= \prod_{j=0}^n \left\{ \sum_{m \geq 3} q_m \left[ x^{m-2} \hat{T}_j^{m-1}(x) + (m-1)x^{m-2} \hat{T}_j^{m-2}(x) \Sigma_j(x) + \left( \sum_{i=0}^{m-3} (i+1)x^i \hat{T}_j^i(x) \right) S_j^2(x) \right] \right. \\ &\quad \left. - (1-p) \prod_{j=0}^n \left\{ \sum_{m \geq 3} q_m \left[ (m-1)x^{m-2} \hat{T}_j^{m-2}(x) \Sigma_j(x) + \left( \sum_{i=0}^{m-3} (i+1)x^i \hat{T}_j^i(x) \right) S_j^2(x) \right] \right\} \right\}, \\ \hat{\Sigma}_{n+1}(x) &= (1-p) \prod_{j=0}^n \left\{ \sum_{m \geq 3} q_m \left[ (m-1)x^{m-2} \hat{T}_j^{m-2}(x) \Sigma_j(x) + \left( \sum_{i=0}^{m-3} (i+1)x^i \hat{T}_j^i(x) \right) S_j^2(x) \right] \right\}, \\ \hat{S}_{n+1}(x) &= (1-p) \prod_{j=0}^n \left\{ \sum_{m \geq 3} q_m \left[ \left( \sum_{i=0}^{m-2} x^i \hat{T}_j^i(x) \right) S_j(x) \right] \right\}.\end{aligned}\quad (16)$$

These equations differ significantly from the corresponding equations valid for two-dimensional hyperbolic manifolds [15,31] and for branched simplicial complexes [16]. In fact these equations for  $\hat{T}_{n+1}(x)$ ,  $\hat{\Sigma}_{n+1}(x)$  and  $\hat{S}_{n+1}(x)$  depend on the entire RG flow of the process, i.e., their left hand side is a function of all  $\hat{T}_j(x)$ ,  $\hat{\Sigma}_j(x)$  and  $\hat{S}_j(x)$  all previous iterations  $j$  with  $0 \leq j \leq n$ .

This apparent complication of the obtained equations can be removed by introducing an auxiliary function  $\hat{K}_{n+1}(x)$  (see, for instance, a similar trick used for the Gaussian model in Refs. [25,26]). To show this let us rewrite Eq. (16) as

$$\begin{aligned}\hat{T}_{n+1}(x) &= \hat{K}_{n+1}(x) - \hat{\Sigma}_{n+1}(x), \\ \hat{K}_{n+1}(x) &= \prod_{j=0}^n \left\{ \sum_{m \geq 3} q_m \left[ x^{m-2} \hat{T}_j^{m-1}(x) + (m-1)x^{m-2} \hat{T}_j^{m-2}(x) \Sigma_j(x) + \left( \sum_{i=0}^{m-3} (i+1)x^i \hat{T}_j^i(x) \right) S_j^2(x) \right] \right\}, \\ \Sigma_{n+1}(x) &= (1-p) \prod_{j=0}^n \left\{ \sum_{m \geq 3} q_m \left[ (m-1)x^{m-2} \hat{T}_j^{m-2}(x) \Sigma_j(x) + \left( \sum_{i=0}^{m-3} (i+1)x^i \hat{T}_j^i(x) \right) S_j^2(x) \right] \right\}, \\ S_{n+1}(x) &= (1-p) \prod_{j=0}^n \left\{ \sum_{m \geq 3} q_m \left[ \left( \sum_{i=0}^{m-2} x^i \hat{T}_j^i(x) \right) S_j(x) \right] \right\},\end{aligned}\quad (17)$$

with initial conditions  $\hat{T}_0(x) = p$ ,  $\hat{\Sigma}_0(x) = \hat{S}_0(x) = 1 - p$ ,  $\hat{K}_0(x) = 1$ . This latter system of equations can be expressed by a set of iterative equations between the variables at iteration  $n$  and the variable at iteration  $n+1$ , i.e.,

$$\begin{aligned}\hat{T}_{n+1}(x) &= \hat{K}_{n+1}(x) - \hat{\Sigma}_{n+1}(x), \\ \hat{K}_{n+1}(x) &= \hat{K}_n(x) \left\{ \sum_{m \geq 3} q_m \left[ x^{m-2} \hat{T}_n^{m-1}(x) + (m-1)x^{m-2} \hat{T}_n^{m-2}(x) \Sigma_n(x) + \left( \sum_{i=0}^{m-3} (i+1)x^i \hat{T}_n^i(x) \right) S_n^2(x) \right] \right\}, \\ \Sigma_{n+1}(x) &= \Sigma_n(x) \left\{ \sum_{m \geq 3} q_m \left[ (m-1)x^{m-2} \hat{T}_n^{m-2}(x) \Sigma_n(x) + \left( \sum_{i=0}^{m-3} (i+1)x^i \hat{T}_n^i(x) \right) S_n^2(x) \right] \right\}, \\ S_{n+1}(x) &= S_n(x) \left\{ \sum_{m \geq 3} q_m \left[ \left( \sum_{i=0}^{m-2} x^i \hat{T}_n^i(x) \right) S_n(x) \right] \right\}.\end{aligned}\quad (18)$$

As we will see in the next section, this recursive set of equations will turn out to be particularly useful for evaluating the expected size of the giant component.

### C. Order parameter

The order parameter of link percolation is the fraction of nodes  $P_\infty$  that in the thermodynamic limit belongs to the giant component, i.e.,

$$P_\infty = \lim_{n \rightarrow \infty} \frac{M_n}{N_n}, \quad (19)$$

where  $M_n$  is the expected size of the giant component connected to the two initial nodes of the cell complex. The value of  $M_n$  can be derived from the generating function  $\hat{T}_n(x)$  by differentiation, i.e.,

$$M_n = \left. \frac{d\hat{T}_n(x)}{dx} \right|_{x=1}. \quad (20)$$

To obtain  $M_n$  we rewrite Eq. (18) in terms of the vector

$$\begin{aligned}\mathbf{V}_n(x) &= [V_n^1(x), V_n^2(x), V_n^3(x), V_n^4(x)]^\top \\ &= [\hat{T}_n(x), \hat{K}_n(x), \hat{\Sigma}_n(x), \hat{S}_n(x)]^\top,\end{aligned}\quad (21)$$

as

$$\mathbf{V}_{n+1}^s(x) = \mathbf{F}_n(\{\mathbf{V}_n(x)\}, x). \quad (22)$$

By using this notation, we note that the derivative of  $\mathbf{V}_{n+1}(x)$  calculated at  $x = 1$  follows

$$\left. \frac{d\mathbf{V}_{n+1}(x)}{dx} \right|_{x=1} = \mathbf{J}_n \left. \frac{d\mathbf{V}_n^p(x)}{dx} \right|_{x=1} + \left. \frac{\partial \mathbf{F}_n^s}{\partial x} \right|_{x=1}, \quad (23)$$

where  $\mathbf{J}_n$  indicates the Jacobian matrix of the system of Eq. (22). The initial condition of Eq. (23) is  $\dot{\mathbf{V}}_0 = \mathbf{0}$  obtained by taking into consideration that the initial nodes are not counted. To evaluate Eq. (22) we need to provide an explicit expression of the Jacobian matrix  $\mathbf{J}_n$  whose elements are given by

$$[\mathbf{J}_n]_{ij} = \left. \frac{\partial F_{n+1}^i}{\partial V_n^j(x)} \right|_{x=1}. \quad (24)$$

Let us we indicate with  $T_n = \hat{T}_n(1)$ ,  $\Sigma_n = \Sigma_n(1)$ ,  $S_n = \hat{S}_n(1)$  and  $K_n = \hat{K}_n(1)$  that by definition satisfy  $T_n = 1 - S_n = 1 - \Sigma_n$  and  $K_n = 1$ .

$$\mathbf{J}_n = \begin{pmatrix} \mathcal{Q}'(T_n) + 2T_n[H(T_n) - \mathcal{Q}'(T_n)] & 1 & T_n\mathcal{Q}'(T_n) - S_nH(T_n) & 2T_n[H(T_n) - \mathcal{Q}'(T_n)] \\ \mathcal{Q}'(T_n) + 2[H(T_n) - \mathcal{Q}'(T_n)] & 1 & \mathcal{Q}'(T_n) & 2[H(T_n) - \mathcal{Q}'(T_n)] \\ 2S_n[H(T_n) - \mathcal{Q}'(T_n)] & 0 & S_n[H(T_n) + \mathcal{Q}'(T_n)] & 2S_n[H(T_n) - \mathcal{Q}'(T_n)] \\ S_n[H(T_n) - \mathcal{Q}'(T_n)] & 0 & 0 & 2S_nH(T_n) \end{pmatrix}. \quad (27)$$

Similarly, the nonhomogeneous term can be expressed as

$$\frac{\partial \mathbf{F}_n}{\partial x} = \begin{pmatrix} (m-2)\mathcal{Q}(T_n) + 2T_n^2(H(T_n) - \mathcal{Q}'(T_n)) \\ (m-2)\mathcal{Q}(T_n) + 2T_n[H(T_n) - \mathcal{Q}'(T_n)] \\ 2T_nS_n[H(T_n) - \mathcal{Q}'(T_n)] \\ T_nS_n[H(T_n) - \mathcal{Q}'(T_n)] \end{pmatrix}.$$

Since we have now an explicit expression for both  $\mathbf{J}_n$  and  $\partial \mathbf{F}_n / \partial x$ , we can numerically integrate Eq. (22) finding the number of nodes  $M_n$  in the giant component of pseudofractal cell complexes for any value of  $n$  (numerical precision permitting). However, we also want to have some analytical predictions of the critical properties of link percolation. To this end we notice that for  $n > 0$  and  $T_n < 1$  the nonhomogeneous term  $\partial \mathbf{F}_n / \partial x$  is subleading with respect to the homogeneous one in Eq. (22). However, for  $n = 0$  the homogeneous term vanishes due to the initial condition  $\dot{\mathbf{V}}_0 = \mathbf{0}$  so therefore the nonhomogeneous term cannot be neglected. Therefore, we can express  $\dot{\mathbf{V}}_{n+1}$  as

$$\dot{\mathbf{V}}_{n+1} \simeq \mathcal{A}_n \prod_{n'=1}^n \lambda_{n'} \mathbf{u}_{n'}, \quad (28)$$

where  $\lambda_n$  and  $\mathbf{u}_n$  are the largest eigenvalue and the corresponding left eigenvector of the Jacobian matrix  $\mathbf{J}_n$  and  $\mathcal{A}_n$  is

$$\mathbf{v}_n = \frac{1}{C^R} \begin{pmatrix} K(\hat{T}_n) - 4H(T_n)(1 - T_n) + \sqrt{\hat{\Delta}(T_n)}2(H(T_n) - \mathcal{Q}'(T_n))(T_n - 1) \\ K(\hat{T}_n) - 4\mathcal{Q}'(T_n)(1 - T_n) + \sqrt{\hat{\Delta}(T_n)} \\ -4(H(T_n) - \mathcal{Q}'(T_n))(T_n - 1) \\ -2(H(T_n) - \mathcal{Q}'(T_n))(T_n - 1) \end{pmatrix}, \quad (32)$$

By direct calculation of the Jacobian  $\mathbf{J}_n$  we notice that  $\mathbf{J}_n$  can be expressed as a function of  $\mathcal{Q}(T_n)$  and  $H(T_n)$  with  $\mathcal{Q}(T)$  given by Eq. (5) and  $H(T)$  given by

$$H(T) = \sum_{m \geq 3} q_m \sum_{i=0}^{m-2} T^i. \quad (25)$$

In fact, by using the following two relations:

$$\begin{aligned} (1 - T_n) \sum_{i=0}^{m-3} i(i+1)T_n^{i-1} \\ = 2 \sum_{i=0}^{m-3} (i+1)T_n^i - (m-1)(m-2)T_n^{m-3} \end{aligned} \quad (26)$$

and

$$(1 - T_n) \sum_{i=0}^{m-3} (i+1)T_n^i = \sum_{i=0}^{m-2} T_n^i - (m-1)T_n^{m-2},$$

and using  $T_n = 1 - S_n = 1 - \Sigma_n$ ,  $K_n = 1$ , a direct calculation shows that  $\mathbf{J}_n$  is given by

given by

$$\mathcal{A}_n = \left( \prod_{n'=2}^n \langle \mathbf{v}_{n'} | \mathbf{u}_{n'-1} \rangle \right) \langle \mathbf{v}_1 | \dot{\mathbf{V}}_1 \rangle, \quad (29)$$

with  $\dot{\mathbf{V}}_0 = \partial \mathbf{F}_0 / \partial x$  and  $\mathbf{v}_n$ , indicating the right eigenvector corresponding to the largest eigenvalue of the Jacobian  $\mathbf{J}_n$ .

Using Eq. (27) we can directly calculate the largest eigenvalue  $\lambda_n$  of the Jacobian matrix  $\mathbf{J}_n$  which is given by

$$\lambda_n = \frac{1}{2} [\hat{K}(T_n) + \sqrt{\hat{\Delta}(T_n)}], \quad (30)$$

where  $\hat{\Delta}(T_n)$  and  $\hat{K}(T_n)$  are given by

$$\begin{aligned} \hat{K}(T_n) &= (1 - 2T)\mathcal{Q}'(T_n) + 2H(T_n) + 1, \\ \hat{\Delta}(T_n) &= [\hat{K}(T_n)]^2 + 8(T-1)[H^2(T_n) + \mathcal{Q}'(T_n)]. \end{aligned} \quad (31)$$

Note that for  $T_n \rightarrow 1$  then  $\lambda_n \rightarrow \langle m \rangle$ .

The right eigenvector  $\mathbf{v}_n$  corresponding to the largest eigenvalue of  $\mathbf{J}_n$  is given by

and the corresponding left eigenvector  $\mathbf{u}_n$  is given by

$$\mathbf{u}_n^L = \frac{1}{C^L} \begin{pmatrix} 2H^3(T_n) + 4H(T_n)Q'(T_n) - 2Q^2(T_n) + H^2(T_n)[-1 - 3Q'(T_n) + 2T_nQ'(T_n) + \sqrt{\hat{\Delta}(T_n)}] \\ 2H^2(T_n) - 2H(T_n)Q'(T_n) + Q'(T_n)[1 - Q'(T_n) + 2T_nQ'(T_n) + \sqrt{\hat{\Delta}(T_n)}] \\ -2H^3(T_n) + 2Q^2(T_n) + H^2(T_n)[-1 + Q'(T_n) + 2T_nQ'(T_n) + \sqrt{\hat{\Delta}(T_n)}] \\ 4([H(T_n) - Q'(T_n)][H^2(T_n) + Q'(T_n)]) \end{pmatrix}, \quad (33)$$

where  $C^R$  and  $C^L$  are normalization constants which guarantee that the right and left eigenvectors have absolute value one. Note that the right and left eigenvectors of  $\mathbf{v}_n$  and  $\mathbf{u}_n$  satisfy by definition

$$\langle \mathbf{v}_n | \mathbf{u}_n \rangle = 1. \quad (34)$$

From Eqs. (28) and (20) it follows that the expected number of nodes  $M_{n+1}$  in the giant component can be expressed as

$$M_{n+1} \simeq \mathcal{A}_n \prod_{n'=1}^n \lambda_{n'} u_n^1, \quad (35)$$

where  $u_n^1$  indicates the first element of the vector  $\mathbf{u}_n$ .

In Sec. V we will use Eq. (35) to derive the critical properties of link percolation on the pseudofractal cell complexes.

#### IV. RG FLOW

In this section we study the RG flow described by Eq. (6) that we rewrite here for convenience,

$$T_{n+1} = 1 - (1 - T_n)[1 - Q(T_n)], \quad (36)$$

with initial condition  $T_0 = p$ . By defining the auxiliary variable

$$y_n = -\ln(1 - T_n), \quad (37)$$

the RG flow described by Eq. (36) can be written as

$$y_{n+1} = G(y_n) = y_n - \ln[1 - Q(1 - e^{-y_n})]. \quad (38)$$

For  $p \ll 1$ , i.e., close to  $p_c = 0$  we can develop Eq. (38) close to  $T = T_c = 0$ ,  $y_c = 0$ . Stopping at the first relevant term in the expansion of  $y_{n+1} - y_n$  we obtain

$$y_{n+1} - y_n = q_{\bar{m}} y_n^{\bar{m}-1}, \quad (39)$$

with initial condition  $y_0 = -\ln(1 - p)$ . Note that in Eq. (39),  $\bar{m}$  indicates the minimum value of  $m$  for which  $q_m > 0$ . By going in the continuous limit and substituting  $y_n$  with a function  $y(n)$ , Eq. (39) can be written as

$$\frac{dy}{dn} = q_{\bar{m}} y^{\bar{m}-1}. \quad (40)$$

By integrating this equation from 0 up to  $n$  we get

$$y = y_0 [1 - n/n_c]^{-1/(\bar{m}-2)}, \quad (41)$$

with

$$n_c = [(\bar{m} - 2) |\ln(1 - p)|^{\bar{m}-2} q_{\bar{m}}]^{-1}. \quad (42)$$

In particular,  $y$  diverges at a finite value of  $n = n_c$ .

From Eq. (41), using

$$1 - T_n \simeq e^{-y_n}, \quad (43)$$

we get the asymptotic scaling valid for  $y \ll 1$  and  $p \ll 1$ ,

$$1 - T_n = (1 - p)^{\theta_n}, \quad (44)$$

with

$$\theta_n = [1 - (\bar{m} - 2) |\ln(1 - p)|^{\bar{m}-2} q_{\bar{m}} n]^{-1/(\bar{m}-2)}. \quad (45)$$

For  $n \ll n_c$  we can make a further approximation and express  $\theta_n$  as

$$\theta_n \simeq \exp[q_{\bar{m}} p^{\bar{m}-2} n]. \quad (46)$$

Therefore, for  $n \ll n_c$

$$y_n = y_0 \exp[q_{\bar{m}} p^{\bar{m}-2} n], \quad (47)$$

with  $y_0 = |\ln(1 - p)|$ .

In Fig. 4 we show the very good agreement between the numerically integrated value of  $y_n$  and the expression given by Eq. (47) for  $n \ll n_c$ .

Finally, we notice that although Eq. (41) is obtained in the limit  $y \ll 1$  we can see from numerical integration of the RG flow that  $y$  retains the structure

$$y = y_0 f(n/n_c). \quad (48)$$

Although the functional form of  $f(n/n_c)$  obtained in the expansion for  $0 < y \ll 1$  [which can be deduced from Eq. (41)] is not exactly close to  $n \simeq n_c$ , from this expansion we can deduce that  $y$  diverges for a finite value of  $n$  of the order of  $n_c$ . In correspondence of this divergence the linking probability  $T_n$  jumps to  $T_n = 1$  (see Fig. 5).

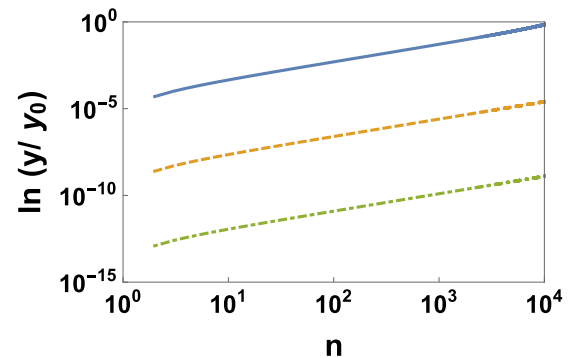


FIG. 4. The RG flow is represented by plotting  $\ln(y/y_0)$  [where  $y_0 = -\ln(1 - p)$ ] versus  $n$  for  $p = 5 \times 10^{-5}$  with  $m = 3$  (blue solid line),  $m = 4$  (orange dashed line), and  $m = 5$  (green dot-dashed line).

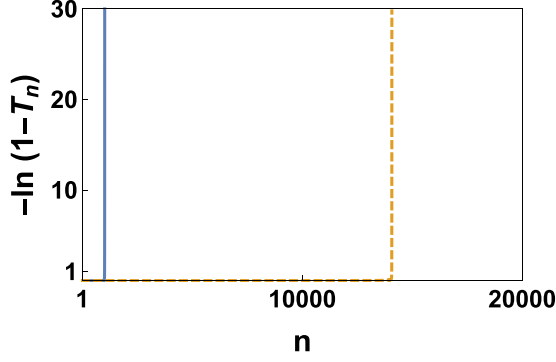


FIG. 5. The RG flow is shown by plotting the value  $y_n = -\ln(1 - T_n)$  where  $T_n$  is the percolation probability, versus  $n$  for fixed value of  $p$ . The solid (blue) line indicates the RG flow for the deterministic pseudofractal simplicial complex with  $m = 3$  and  $p = 10^{-3}$ , the dashed (orange) line indicates the RG flow for the deterministic pseudofractal cell complex with  $m = 4$  and  $p = 6 \times 10^{-3}$ . The divergence of  $y_n$  occurring at a value of  $n$  of the order of magnitude of  $n_c$  is clearly noticeable, indicating that  $T_n$  reaches the value  $T_n = 1$  discontinuously at a finite  $n \simeq n_c$ .

## V. CRITICAL PROPERTIES OF THE ORDER PARAMETER

### A. Critical region

We are interested in characterizing the properties of the order parameter

$$P_\infty = \lim_{n \rightarrow \infty} \frac{M_n}{N_n}, \quad (49)$$

in the critical region, i.e., close to the percolation threshold  $p_c = 0$  taking  $0 < p \ll 1$ . To this end we first discuss the properties of the expected number of nodes  $M_n$  in the giant component when the pseudofractal cell complex has evolved up to iteration  $n$ . According to the derivation obtained in Sec. III C, using Eq. (35),  $M_n$  can be approximated as

$$M_n \simeq \mathcal{A}_{n-1} \prod_{n'=1}^{n-1} \lambda_{n'} u_n^1, \quad (50)$$

where  $\mathcal{A}_n$  is given by Eq. (29), which can be written also as

$$\mathcal{A}_n = \mathcal{D}_n \langle \mathbf{v}_1 | \dot{\mathbf{V}}_1 \rangle, \quad (51)$$

where  $\mathcal{D}_n$  is given by

$$\mathcal{D}_n = \prod_{n'=2}^n \langle \mathbf{v}_{n'} | \mathbf{u}_{n'-1} \rangle. \quad (52)$$

For  $p \simeq p_c$ ,  $\mathcal{D}_n$  is in first approximation independent of  $n$  and approximately equal to one, as the right and left eigenvectors will change slowly with  $n$  and by definition Eq. (34) is satisfied. Therefore, Eq. (50) can be written as

$$M_n \simeq \langle \mathbf{v}_1 | \dot{\mathbf{V}}_1 \rangle \prod_{n'=1}^{n-1} \lambda_{n'} u_n^1. \quad (53)$$

### B. Critical expansions

Our major goal is to study the critical behavior of the order parameter  $P_\infty$  [given by Eq. (49)], depending on the scaling of

the expected number of nodes  $M_n$  [whose leading behavior is given by Eq. (53)] in the pseudofractal simplicial complex with the number of iterations  $n$ .

To this end in this paragraph we will investigate the scaling of  $\lambda_n$  with  $n$  for  $0 < p \ll 1$  and we will investigate the scaling of the other factors  $\langle \mathbf{v}_1 | \dot{\mathbf{V}}_1 \rangle$  and  $u_n^1$  present in Eq. (53) with  $p$ .

The leading eigenvalue  $\lambda_n$  of the Jacobian matrix  $\mathbf{J}_n$  is expressed according to Eq. (30) as a function of  $H(T_n)$  and  $Q(T_n)$ . For  $y_n = -\ln(1 - T_n) \ll 1$  we can expand both  $H(T_n) = H(1 - e^{-y_n})$  and  $Q'(T_n) = Q'(1 - e^{-y_n})$  getting

$$Q'(1 - e^{-y_n}) = q_{\bar{m}}(\bar{m} - 1)y_n^{\bar{m}-2} + \mathcal{O}(y_n^{\bar{m}-1}),$$

$$H(1 - e^{-y_n}) = 1 + y_n + \mathcal{O}(y_n^2), \quad (54)$$

where  $\bar{m}$  indicates the smallest value of  $m$  for which  $q_m > 0$ . Using this expansion in Eq. (30) for the maximum eigenvalue  $\lambda_n$  of the Jacobian matrix, we get

$$\lambda_n = 2(1 + y_n) + \mathcal{O}(y_n^2). \quad (55)$$

For  $y_n \ll 1$  also the inhomogeneous term  $\partial \mathbf{F}_n / \partial x$  can be expanded to give

$$\frac{\partial \mathbf{F}_n}{\partial x} \simeq \begin{pmatrix} (2 + q_3)y_n^2 \\ 2y_n \\ 2y_n \\ y_n \end{pmatrix}, \quad (56)$$

For  $n = 0$  where the homogeneous term vanishes due to the trivial initial condition  $\dot{\mathbf{V}}_0 = \mathbf{0}$  and the inhomogeneous term has the leading behavior

$$\dot{\mathbf{V}}_1 = \frac{\partial \mathbf{F}_0}{\partial x} \simeq \begin{pmatrix} (2 + q_3)p^2 \\ 2p \\ 2p \\ p \end{pmatrix}. \quad (57)$$

Moreover, the leading term of  $\mathbf{v}_1$  is

$$\mathbf{v}_1 \simeq \frac{1}{6 - 4p/3} [(1 + p), (1 - p), (-1 + p), 2]. \quad (58)$$

Therefore, for  $p \ll 1$  we have that  $\langle \mathbf{v}_1 | \dot{\mathbf{V}}_1 \rangle$  scales linearly with  $p$ . In particular,

$$\langle \mathbf{v}_1 | \dot{\mathbf{V}}_1 \rangle \simeq \frac{p}{3}. \quad (59)$$

Finally, we observe that for  $n \gg 1$  we have  $T_n \simeq 1$  and the right eigenvector corresponding to the largest eigenvalue scales like

$$\mathbf{u}_n = (1, 1, 0, 0)^\top. \quad (60)$$

By considering the scaling relations determined by Eqs. (59) and (60) in Eq. (53), we obtain that for  $n \gg 1$  the fraction of nodes  $M_n$  in the giant component obeys

$$M_n \propto p \prod_{n'=1}^{n-1} \lambda_{n'}, \quad (61)$$

with  $\lambda_n$  following Eq. (55) for  $y_n \ll 1$ .

### C. Critical scaling of the order parameter

In this paragraph we derive the asymptotic behavior of the order parameter  $P_\infty$  given by Eq. (49) close to the percolation



threshold  $p_c = 0$ . By approximating  $M_n$  with Eq. (61) the order parameter  $P_\infty$  given by Eq. (49) can be easily shown to obey for  $0 < p \ll 1$ ,

$$\begin{aligned} P_\infty &\propto p \lim_{n \rightarrow \infty} \frac{1}{N_n} \prod_{n'=1}^n \lambda_{n'} \\ &= p \exp \left[ -\ln \langle m \rangle \int_0^\infty dn (1 - \psi_n) \right], \end{aligned} \quad (62)$$

where  $\psi_n$  is defined as

$$\psi_n = \frac{\ln \lambda_n}{\ln \langle m \rangle}. \quad (63)$$

Using for  $\lambda_n$  the expansion given by Eq. (55),  $\psi_n$  can be expanded to give

$$\psi_n = \frac{\ln \lambda_n}{\ln \langle m \rangle} = \frac{\ln 2}{\ln \langle m \rangle} + \frac{y_n}{\ln \langle m \rangle} + O(y_n^2). \quad (64)$$

Therefore, in the continuous limit for  $n$  we get

$$1 - \psi \simeq 1 - \frac{\ln 2}{\ln \langle m \rangle} - \frac{y}{\ln m}, \quad (65)$$

with the function  $y(n)$  given by the scaling function Eq. (48) and diverging for  $n = n_c$ . At a value of  $n \sim n_c$ ,  $T_n$  jumps to  $T_n = 1$ ,  $\lambda_n = \langle m \rangle$ . Consequently, we have that  $1 - \psi_n$  will also have a discontinuity at  $n_c$ , i.e.,

$$1 - \psi_n = \begin{cases} f_\psi(\hat{n}/n_c) & \text{for } n < n_c \\ 0 & \text{for } n > n_c \end{cases}, \quad (66)$$

where  $f_\psi(x)$  is a scaling function. Using this expression in Eq. (62) we obtain

$$\begin{aligned} P_\infty &\propto p \exp \left[ -\ln \langle m \rangle \int_0^\infty dn (1 - \psi_n) \right] \\ &= p \exp \left[ -\ln \langle m \rangle \int_0^{\hat{n}_c} d\hat{n} f_\psi(\hat{n}/n_c) \right]. \end{aligned} \quad (67)$$

By changing the variable of integration from  $n$  to  $x = n/n_c$ , we obtain

$$P_\infty \propto p \exp \left[ -n_c \ln \langle m \rangle \int_0^1 dx f_\psi(x) \right]. \quad (68)$$

Finally, using the expression for  $n_c$  given by Eq. (42), by indicating with  $\alpha$  the constant

$$\alpha = \frac{\ln \langle m \rangle}{(\bar{m} - 2)q_{\bar{m}}} \int_0^1 f_\psi(x) dx, \quad (69)$$

we obtain

$$P_\infty \propto p \exp \left( -\frac{\alpha}{|\ln(1-p)|^{\bar{m}-2}} \right). \quad (70)$$

Because in the critical region  $p \ll 1$ , it follows that  $P_\infty$  follows the asymptotic scaling

$$P_\infty \propto p \exp(-\alpha/p^{\bar{m}-2}). \quad (71)$$

This scaling can be validated by numerically integrating Eq. (23) and using the finite size scaling of  $P_n$  defined as the fraction of nodes in the giant component of a pseudofractal

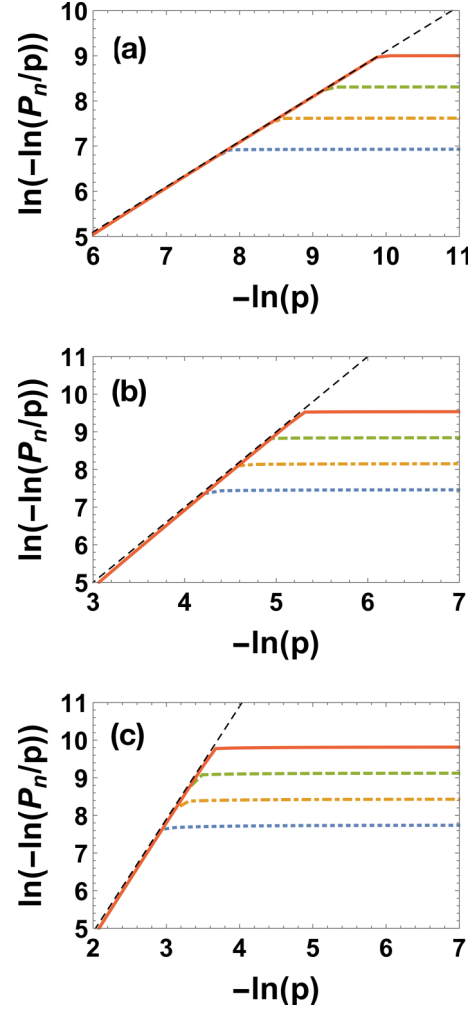


FIG. 6. The scaling of the order parameter  $P_n$  is shown as a function of  $p$  for the deterministic pseudofractal simplicial and cell complexes with  $m = 3$  (top panel),  $m = 4$  (central panel), and  $m = 5$  (bottom panel). The order parameter  $P_n$  is shown for different values of  $n = 20\,000$ ,  $10\,000$ ,  $5\,000$ ,  $2\,500$  indicated with solid (red), dashed (green), dot-dashed (orange), and dotted (blue) thick lines. The predicted scaling of the order parameter in the infinite network limit is indicated with the thin dashed (black) line.

cell complexes evolved up to iteration  $n$ , i.e.,

$$P_n = \frac{M_n}{N_n}. \quad (72)$$

Our numerical results shown in Fig. 6 clearly demonstrates that if  $n > n_c$  [where  $n_c$  is a function of  $p$  defined by Eq. (42)] then  $P_n$  follows the asymptotic scaling defined in Eq. (71). However, if  $n < n_c$ , then  $P_n$  saturates to a constant value. This phenomenology is in perfect agreement with our theoretical understanding of the critical properties of link percolation on pseudofractal cell complexes.

## VI. CONCLUSIONS

In this work we have studied the nature of the link percolation transition in pseudofractal simplicial and cell complexes. The pseudofractal generalized networks under

study include deterministic and random cell complexes, made by gluing together  $m$ -polygons with the same number of sides  $m$  or with random number of sides  $m$  drawn from a  $q_m$  distribution. All these generalized network topologies display a link percolation transition at  $p_c = 0$ . However, the critical behavior of the order parameter depends on the topology of the generalized network structure. For deterministic pseudofractal simplicial complexes ( $m = 3$ ) we confirm the results of Ref. [42] showing that the order parameter is exponentially suppressed by a term  $1/p$  and we predict an additional modulation of the order parameter by a factor  $p$ . For deterministic pseudofractal cell complexes with  $m > 3$  we show that the exponential suppression is more severe than for simplicial complexes and decays as  $1/p^{m-2}$ . Finally, for random cell complexes we show that the critical behavior is dominated by

the smallest value of  $m$ ,  $\bar{m}$  for which  $q_m > 0$ . It follows that albeit both simplicial and cell complexes have an order parameter that is exponentially suppressed close to the critical point, the universality of the phase transition is weakened by the dependence on  $m$  of this exponential suppression. Therefore in this work shows clearly that the dynamical processes defined on simplicial complexes and their cell complex counterpart might be significantly different, emphasizing the important role that network topology and geometry have on dynamical processes.

#### ACKNOWLEDGMENT

H.S. acknowledges support from the China Scholarship Council.

- 
- [1] G. Bianconi, *Europhys. Lett.* **111**, 56001 (2015).
- [2] V. Salnikov, D. Cassese, and R. Lambiotte, *Euro. J. Phys.* **40**, 014001 (2018).
- [3] C. Giusti, R. Ghrist, and D. S. Bassett, *J. Comput. Neurosci.* **41**, 1 (2016).
- [4] G. Petri, P. Expert, F. Turkheimer, R. Carhart-Harris, D. Nutt, P. J. Hellyer, and F. Vaccarino, *J. Roy. Soc. Interface* **11**, 20140873 (2014).
- [5] M. W. Reimann, M. Nolte, M. Scolamiero, K. Turner, R. Perin, G. Chindemi, P. Dłotko, R. Levi, K. Hess, and H. Markram, *Front. Comput. Neurosci.* **11**, 48 (2017).
- [6] G. Petri and A. Barrat, *Phys. Rev. Lett.* **121**, 228301 (2018).
- [7] I. Iacopini, G. Petri, A. Barrat, and V. Latora, *Nat. Comm.* **10**, 2485 (2019).
- [8] U. Alvarez-Rodriguez, F. Battiston, G. F. de Arruda, Y. Moreno, M. Perc, and V. Latora, *arXiv:2001.10313* (2020).
- [9] L. Papadopoulos, M. A. Porter, K. E. Daniels, and D. S. Bassett, *J. Complex Networks* **6**, 485 (2018).
- [10] M. Šuvakov, M. Andjelković, and B. Tadić, *Sci. Rep.* **8**, 1 (2018).
- [11] Z. Wu, G. Menichetti, C. Rahmede, and G. Bianconi, *Sci. Rep.* **5**, 10073 (2015).
- [12] G. Bianconi and C. Rahmede, *Sci. Rep.* **7**, 41974 (2017).
- [13] D. Mulder and G. Bianconi, *J. Stat. Phys.* **173**, 783 (2018).
- [14] G. Bianconi and R. M. Ziff, *Phys. Rev. E* **98**, 052308 (2018).
- [15] I. Kryven, R. M. Ziff, and G. Bianconi, *Phys. Rev. E* **100**, 022306 (2019).
- [16] G. Bianconi, I. Kryven, and R. M. Ziff, *Phys. Rev. E* **100**, 062311 (2019).
- [17] T. Hasegawa and K. Nemoto, *Phys. Rev. E* **88**, 062807 (2013).
- [18] P. S. Skardal and A. Arenas, *Phys. Rev. Lett.* **122**, 248301 (2019).
- [19] A. P. Millán, J. J. Torres, and G. Bianconi, *Phys. Rev. Lett.* **124**, 218301 (2020).
- [20] L. V. Gambuzza, F. Di Patti, L. Gallo, S. Lepri, M. Romance, R. Criado, M. Frasca, V. Latora, and S. Boccaletti, *arXiv:2004.03913* (2020).
- [21] M. Lucas, G. Cencetti, and F. Battiston, *arXiv:2003.09734* (2020).
- [22] A. P. Millán, J. J. Torres, and G. Bianconi, *Sci. Rep.* **8**, 9910 (2018).
- [23] A. P. Millán, J. J. Torres, and G. Bianconi, *Phys. Rev. E* **99**, 022307 (2019).
- [24] G. St-Onge, V. Thibeault, A. Allard, L. J. Dubé, and Hébert-Dufresne, *arXiv:2004.10203* (2020).
- [25] G. Bianconi and S. N. Dorogovstev, *J. Stat. Mech.: Theor. Exp.* (2020) 014005.
- [26] M. Reitz and G. Bianconi, *arXiv:2003.09143* (2020).
- [27] J. J. Torres and G. Bianconi, *J. Phys. Complexity* **1**, 015002 (2020).
- [28] T. Carletti, F. Battiston, G. Cencetti, and D. Fanelli, *Phys. Rev. E* **101**, 022308 (2020).
- [29] A. A. Migdal, *Sov. J. Exp. Theor. Phys.* **42**, 743 (1976).
- [30] L. P. Kadanoff, *Ann. Phys.* **100**, 359 (1976).
- [31] S. Boettcher, V. Singh, and R. M. Ziff, *Nat. Comm.* **3**, 787 (2012).
- [32] S. Boettcher, J. L. Cook, and R. M. Ziff, *Phys. Rev. E* **80**, 041115 (2009).
- [33] T. Nogawa, *J. Phys. A: Math. Gen.* **51**, 505003 (2018).
- [34] T. Hasegawa, M. Sato, and K. Nemoto, *Phys. Rev. E* **82**, 046101 (2010).
- [35] T. Nogawa and T. Hasegawa, *Phys. Rev. E* **89**, 042803 (2014).
- [36] D. M. Auto, A. A. Moreira, H. J. Herrmann, and J. S. Andrade Jr., *Phys. Rev. E* **78**, 066112 (2008).
- [37] S. Boettcher and C. T. Brunson, *Europhys. Lett.* **110**, 26005 (2015).
- [38] V. Singh, C. T. Brunson, and S. Boettcher, *Phys. Rev. E* **90**, 052119 (2014).
- [39] S. Boettcher and C. T. Brunson, *Phys. Rev. E* **83**, 021103 (2011).
- [40] M. Hinczewski and A. N. Berker, *Phys. Rev. E* **73**, 066126 (2006).
- [41] S. N. Dorogovtsev, A. V. Goltsev, and J. F. F. Mendes, *Phys. Rev. E* **65**, 066122 (2002).
- [42] S. N. Dorogovtsev, *Phys. Rev. E* **67**, 045102(R) (2003).